euspen's 22nd International Conference & Exhibition, Geneva, CH, May/June 2022
www.euspen.eu

Ductile cutting regime in ball milling of single crystal silicon

Marvin Groeb[1,2], Yannik Zecha[3], Johann Groeb[4], Matthias Fritz[2], Wolfgang Ensinger[1]

[1]*Department of Materials Science, Technical University of Darmstadt,* [2]*Kern Microtechnik GmbH, Eschenlohe,* [3]*Zecha Hartmetall-Werkzeugfabrik GmbH, Königsbach-Stein,* [4]*Independent Researcher, Darmstadt*

Marvin.groeb@Kern-microtechnik.com

Abstract
The requirements to surface finish, but also surface composition in the mechanical finishing of monocrystalline silicon are high and constantly increasing. Traditionally, optical surfaces are ground and then lapped to specification often reaching a surface roughness in the single digit nanometre range. Increasingly complex shapes, the need for high accuracy as well as the need for higher productivity and decreasing costs require novel approaches towards mechanical finishing. In this study, commercially available semiconductor-grade monocrystalline silicon is machined on a high precision milling machine with monocrystalline diamond tooling. A series of experiments are undertaken, varying the relevant process parameters such as type of tooling, depth of cut, cutting speed, stepdown and chip thickness. A Taguchi based design of experiments is used to reduce the number of experiments, with the aim of achieving a ductile cutting regime. The results are analysed with an ANOVA analysis. For this, the milled surfaces are characterised in process via an acoustic emission sensor. The milled surfaces are analysed via confocal laser scanning microscopy and the ISO 25178 areal surface quality parameters such as Sa, Sq are determined. Furthermore, the areal material ratio Smr is used to quantify the intact surface ratio. Scanning electron microscopy is used to qualitatively characterize the surfaces, but also to identify surface damages such as grooves, breakouts and pitting. The specimen exhibits a high gloss and reflectance. The undamaged surface in combination with a small median chip thickness is indicative of a ductile cutting regime.

Milling, diamond, ductile cutting regime, mirror finishing, silicon

1. Introduction

In 2012, the optical elements market was estimated at $3.6 billion and is expected to grow to $12.3 billion by 2019 [1]. Growing demands on the workpiece surface increase the cost of machine tools, tooling, and machining time. Monocrystalline silicon is chosen as a lens material for IR and X-ray applications due to its low thermal expansion, low density, and relatively low cost [2]. Furthermore, it is one of the building blocks of today's semiconductor technology [3].
Currently, chemical or mechanical polishing [4], [5], lapping [6], [7]or diamond turning [8], [2] can achieve high quality surface [9], [10] for quality control of packaged chips by ultrasonic microscopy.
Single-point diamond turning (SPDT) has been using the transition phenomenon from brittleness to ductility [11], [12] to achieve high-quality surfaces in brittle, hard materials.
Unfortunately, this process is characterized by low productivity, high part cost, [13] and limited dimensional freedom due to the accessibility of the diamond tool.
For a number of brittle materials, such as germanium, [14] glass, [15] as well as softer non-ferrous materials, e.g. aluminium, [16] mirror-finish milling has been possible with monocrystalline diamond tools. Recently, a ductile cutting regime superfinishing in both face and side milling of monocrystalline silicon has been shown [17]. As wafer thickness is constantly decreasing, chips are prone to warping. In order to analyse packaged chips, a freeform superfinishing process is needed. The following papers aims at transferring the ductile cutting process towards freeform milling.

2. Methodology & Experimental

The milling experiments were conducted on a Kern Micro HD precision CNC machining centre. The machine has linear guideways with micro gap hydrostatic bearing surfaces, linear motors, and glass scales with nanometric resolution, which enables a positioning control well below 1 µm and constant feed rates with low vibrations. The machine is equipped with an HSK 40 high speed spindle (42000 min^{-1}, 15.6 kW) manufactured by Fischer, CH. The sample specimen (semiconductor grade commercial monocrystalline Si wafers, 700µm thickness) were superglued to a face milled piece of aluminium (EN AWT 5081). Roughing was performed with a 8 mm polycrystalline diamond (PCD) tool (Dixi Polytools, CH), and semi finishing with a 6 mm PCD ball endmill (Matzdorf, GER). The used NC code was written in Heidenhain plain text on the TNC 640 control. A contour smoothing cycle of 0.0005 mm was active during the operation. The milling was performed under flood coolant, the coolant used is a GTL oil (Oelheld SintroGrind TC-X 1500). The finishing was performed with both a 6 mm monocrystalline diamond (MCD) ball endmill (Contour Fine Diamonds, NL) as well as the 6 mm PCD ball endmill from the semi finishing operation. The tools were held in Regofix PowRgrip toolholders, runout was verified to less than 2 µm after setting the tool. Tests were performed in a temperature-controlled environment. Before taking a cut, a spindle warm-up period of 300 seconds was completed. To further reduce thermal influences, the work piece temperature was stabilized by applying tempered flood coolant for 10 minutes before the experiment. Measurements were taken after cleaning the sample in an ultrasonic bath with isopropyl alcohol. All quantitative measurements were recorded with a

Confovis Duo Vario confocal laser scanning microscope (CLSM), whereas qualitative analysis was done with a Thermo Fischer Phenom XL scanning electron microscope (SEM).

In order to achieve comparable experimental results, the sample specimen was prepared identically. For this, the aluminium fixture is machined flat with a generic DLC coated endmill. A level surface (flatness < 1 µm) with a roughness of Sa 0.15 µm was achieved. After milling, the surface is cleaned with isopropyl alcohol and the sample specimen is superglued (Ergo 5210) to the aluminium surface. A weight of 100 g is placed on the specimen during hardening to ensure contact. The sample specimen is located with the built-in touch probe (Blum TC 52 LF). The tools are measured after chemical cleaning with the equipped Blum LC50 laser. Runout is verified via the laser to better than 1 µm on the shaft directly above the cutting edge. To account for unwanted thermal expansion of the spindle, a warm-up period of 300 s is performed before measuring.

2.1 Design of Experiments

A Taguchi-based Design of Experiment approach was used in the planning of the experiment series. In order to limit the time per parameter set to an acceptable timeframe, the width of cut (distance between two parallel passes) was chosen based on a numeric calculation of the cusp height (less than 5 nm) and fixed at 0.009 mm. A first experiment series, undertaken with a 6 mm ball endmill (angulation: 45°) was performed by varying the cutting speed, the median chip thickness, and the depth of cut along 4 levels. A second experiment series explores the relationship between cutting speed and median chip thickness with a PCD tool. Table 1 lists the analysed parameters in the two experiment series.

Table 1: The parameters for the two experiment series

Parameter	Experiment 1	Experiment 2
Parameter 1	Cutting Speed (Vc)	Cutting Speed (Vc)
Parameter 2	Median Chip Thickness (Hm)	Median Chip Thickness (Hm)
Parameter 3	Depth of Cut (DOC)	-

Because the endmill is kept at a low radial engagement, the median chip thickness is much lower than the calculated feed per tooth. It is calculated via equation 1. [18] Here, the median chip thickness (H_m) is a function of the engagement angle (φ), the stepover (a_e), the diameter of the tool (D) and the feed per tooth (F_z).

$$H_m = \frac{114.6}{\varphi} * \frac{a_e}{D} * F_z \qquad (1)$$

For testing purposes, a flat surface is milled with parallel offset passes. This enables an easier analysis with optical instruments, and also shows qualitative errors in visual inspection, moreover reducing the influence of machine positioning errors by only having a single moving axis at a time. The transfer from a planar, ball milled surface towards lightly curved surfaces is usually trivial.

2.2 First experiment series - MCD

The parameters cutting speed, depth of cut and median chip thickness have the most significant influence towards achieving a ductile cutting regime. For this reason, a scoping experiment is undertaken, exploring their relationship in the ball milling of monocrystalline silicon. Table 2 lists the analysed parameters as well as their corresponding levels. A fully orthogonal test matrix (T16) was used.

Table 2: The analysed parameters and their corresponding levels in the first experiment series.

Parameter	Level 1	Level 2	Level 3	Level 4
Vc in m/min	138.06	276.12	414.19	552.25
Hm in nm	10	20	40	100
DOC in µm	0.5	1	1.5	2

The cutting speed Vc is the actual cutting speed at the engagement point of the spherical tool with an angulation of 45°. Especially in regard to the lower depth of cut levels, two offset passes were milled at 2 µm depth of cut to ensure an accurate final pass at the stated depth.

The cutting speed was chosen to fit within the lower (10000 min^{-1}) and upper end (40000 min^{-1}) of the sensibly available spindle rotational speed. During the experiment, acoustic emission data is recorded. The recorded data is transformed via an FFT (method: Welch, window: 2048) into a PSD (power spectral density). The integral of the PSD is used as a quality criterion. After cleaning in isopropyl alcohol and drying in vacuum exicator, the samples are analysed in the SEM and CLSM. In addition to a qualitative visual inspection of the surface, the optically measured arithmetic areal surface roughness (Sa), the quadratic areal surface roughness (Sq) and the areal material ratio (Smr) are calculated from the CLSM data.

2.3 Second experiment series - PCD

The second experiment series analysed the cutting parameters cutting speed and chip thickness. Because the first experiment series already explored the cutting depth, it was fixed at 2 µm. Moreover, the cutting speed was limited towards low noise rotational speeds on the high-speed spindle. A PCD tool (6 mm diameter, ball endmill) was used. Table 3 lists the analysed parameters for the second experiment series. A fully orthogonal test matrix (T10) was used to build up the experiment.

Table 3: The analysed parameters and their corresponding levels in the second experiment series.

Parameter	Level 1	Level 2	Level 3	Level 4	Level 5
Vc in m/min	351.89	492.64			
Hm in nm	10	20	40	80	160

The cleaned samples are analysed in an identical fashion to the first experiment series.

3. Results and Discussion

The first experiment series showed a matte, smooth surface in visual inspection. Figure 1 shows the achieved surface roughness Sa and Sq and the corresponding median chip thickness, whereas Figure 2 shows the achieved surface roughness in relation to the cutting speed. An ANOVA analysis shows that no single factor has a large influence over the whole experiment series (see Table 4). The correlation of the parameters (R-squared) towards the quality parameter is unindicative of a close correlation. A correlation of the recorded AE data is inconclusive regarding an ANOVA analysis. The sum of the PSD data correlates with the recorded roughness data, although the correlation is not very strong (0.45). Due to scarcity of the

paper's length, the authors refrained from printing the corresponding chart.

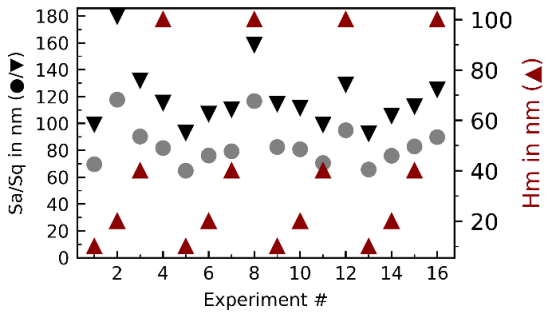

Figure 1: The areal surface roughness parameters at different median chip thickness in the first experiment series.

Taking a closer look, it can be seen that especially at median and high cutting speeds (compare Figure 2), the roughness increases with higher median chip thicknesses, thus forming the base for the chosen cutting speed in the second experiment series. A likely explanation why this effect is absent at the lower cutting speeds is the initial wear behaviour on the MCD tool, introducing a lot of nonlinear deviations into the results, but also tool-workpiece vibrations at certain frequencies.

Table 4: The ANOVA analysis for the firsts experiment series. The roughness parameter Sq was chosen as a quality parameter.

	Sum_sq	Pr(>F)
Vc	1.02E-03	0.177
Hm	1.23E-03	0.141
DOC	4.57E-07	0.976
R-squared	0.274	

Figure 4 shows SEM micrographs of the created surfaces. It can be seen that the surface has certain areas with surface defects (a, c) and certain areas show a lower amount of surface damage. Analysing the surface with the areal surface roughness parameters such as Sa, Sq is a good indicator for overall smoothness, but gives little information on how the surface is composed. Mathematically, the height difference between lowest and highest point has a much larger influence on these values than the overall structure and width of the defects. The ISO 25178 offers a plethora of different parameters to describe the surface.

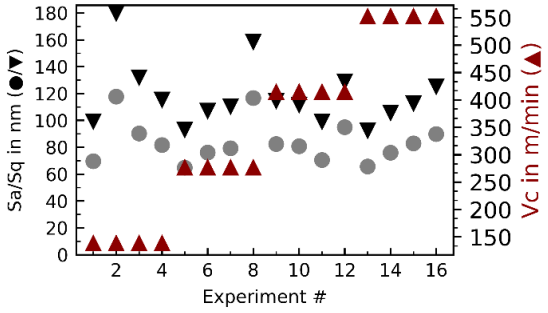

Figure 2: The areal surface roughness parameters at different cutting speeds in the first experiment series.

Parameters such as the auto correlation length (Str) do not produce a sensible result on shallow, fine structures, whereas the areal material ratio, Smr does show a surprisingly good fit towards analysing a surface in regard to the cutting mode. Generally speaking, the roughness of a surface is mostly defined by the tool sharpness and radius waviness, while breakouts in the surface have a low impact, whereas the parameters Smr is drastically altered by larger or more common breakouts.

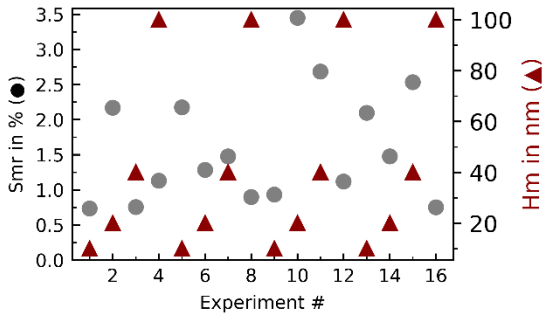

Figure 3: The areal material ratio at different median chip thickness in the first experiment series.

It is clear, that a fully ductile cutting regime was not achieved during the first experiment series, as the surface roughness, areal material ratio but also the qualitative look of the surface (see Figure 4, a-c) show clear brittle fractures and large variations without any correlation towards the median chip thickness. Most likely, the rake angle of the tool at 0° is not negative enough to induce enough hydrostatic stress. During SEM observation of the results, the semi-finished regions (Figure 4d) show a clear ductile cut behaviour, as a metal-like side flow of the material can be seen in the form of prows. For this reason, the second experiment series focused on milling not with a MCD tool, but the PCD ball endmill form semi finishing.

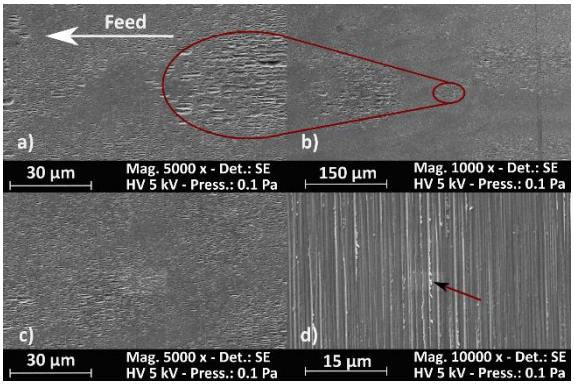

Figure 4: SEM micrographs of 3 areas of interest in the first experiment series: Highest surface roughness at a) 5000x magnification b) 1000x magnification. c) lowest achieved surface roughness, 5000x magnification d) semi-finishing with PCD tool at 10000x magnification. Note the metal like, ductile side flow of the material.

The second experiment series showed a slightly glossy surface with regular, visible feed lines. The surface roughness is roughly 20 nm lower than on the first experiment series, with a lower variation (see Figure 5). The areal material ratio (Figure 6) clearly distinguishes between flawless milled parameter sets (see Figure 7 a-b) whereas a too high median chip thickness leads towards very high Smr values (Figure 7 c-d).

Table 5: The ANOVA analysis for the second experiment series. The areal material ratio Smr was chosen as a quality parameter.

	sum_sq	Pr(>F)
Vc	111.14	0.073879
Hm	1056.527	0.000342
R-squared	0,869	

A conducted ANOVA analysis (quality parameter: Smr) shows a strong influence of the median chip thickness with a very high correlation (R-squared 0.869).

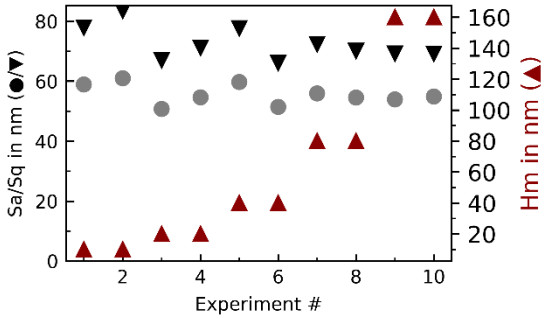

Figure 5: The areal surface roughness parameters at different median chip thickness in the second experiment series.

It can be seen, that the surface roughness (Figure 5) does not vary significantly during the experiment series, most likely because the lower sharpness PCD tool is clearly imprinting (compare Figure 7) the cutting edge waviness onto the sample surface.

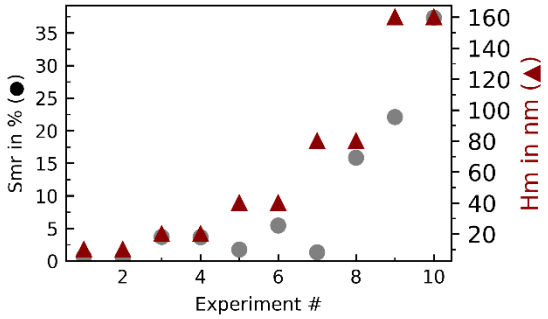

Figure 6: The areal material ratio at different median chip thickness in the second experiment series.

The low Smr values at a median chip thickness below 40 nm as well as the qualitative surface under the scanning electron microscope point towards a ductile cutting regime, matching previous research while face milling [17].

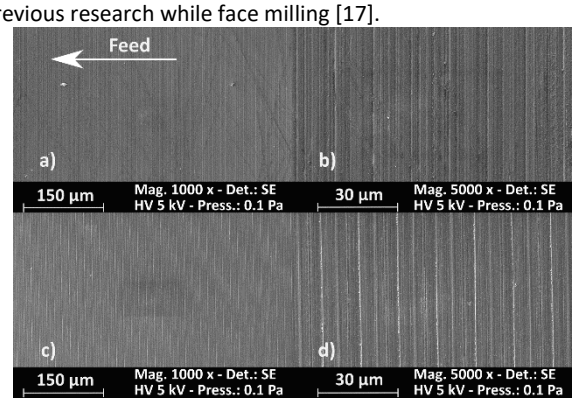

Figure 7: SEM micrographs at two magnifications of: a-b) the parameter set with the lowest Smr c-d) the parameter set with the highest Smr

4. Conclusion

The milled samples exhibit a matte (MCD) and glossy (PCD) surface. The surface roughness, but also a qualitative analysis under the scanning electron microscope point towards a ductile cutting regime, if the median chip thickness stays below 40 nm as no surface damage is visible. The conducted ANOVA analysis shows a significant influence from the median chip thickness. Further experiments should be conducted with a MCD tool with negative rake, enabling a ductile cutting regime while lowering the surface roughness because of a decreased cutting edge radius and waviness.

Figure 8: The milled sample. The ball end milled region is highlighted with a red square. Note the much clearer reflection in this area compared to the rest of the sample specimen.

References

[1] W. G. Research, „Optical Components: Market share, strategies and Forecasts, Worldwide 2013-2019," Massachusetts, 2013.

[2] X. L. R. L. R. S. Goel, „Wear mechanism of diamond tools against single crystal silicon in single point diamond turning process," *Tribology International,* pp. 272-281, 2013.

[3] S. Zhang, „Review of modern field effect transistor technologies for scaling," *Journal of Physics: Conference Series,* 2020.

[4] L. C. Y. Zhao, „A micro-contact and wear model for chemical-mechanical polishing of silicon wafers," *Wear,* 2002.

[5] C. Teichert, „Comparison of surface roughness of polished silicon wafers measured by light scattering topography, soft x-ray scattering and atomic-force microscopy," *Applied Physics Letters,* 1995.

[6] H. Young, „Surface integrity of silicon wafers in ultra precision machining," *The International Journal of Advanced Manufacturing Technology,* 2006.

[7] S. Ozturk, „Optimization of lapping processes of silicon wafer for photovoltaic applications," *Solar Energy,* 2018.

[8] T. Leung, „Diamond turning of silicon substrates in ductile-regime," *Journal of Materials Processing Technology,* 1998.

[9] A. Phommahaxay, „Defect detection in through silicon vias by GHz scanning accoustic microscopy: Key ultrasonic Characteristics, " *IEEE 64th Electronic Components and Technology Conference,* 2014.

[10] W. Dallas, „Resonance ultrasonic vibrations for crack detection in photovoltaic silicon wafers," *Measurement Science and Technology,* 2007.

[11] P. N. Blake, „Ductile Regime machining of germanium and silicon," *Journal of the American Ceramic Society,* 1991.

[12] T. Shibata, „Ductile-regime turning mechanism of single-crystal silicon," *Precision Engineering,* 1996.

[13] Z. Zhang, „Manufacturing technologies towards extreme precision," *Journal of extreme Manufacturing,* 2019.

[14] B. S. Dutterer, „Diamond milling of an alvarez lens in Germanium," *Precision Engineering,* 2014.

[15] Y. Takeuchi, „Ultraprecision 3d micromachining of glass," *CIRP Annals,* 1996.

[16] S. Wang, „An investigation on surface finishing in ultra-precision raster milling of aluminium alloy 6061," *Proceedings of the Institution of Mechanical Engineers,* 2014.

[17] M. Groeb, „Ductile Cutting regime in Diamond Milling of Monocrystalline Silicon," *Proceedings of the 36th Annual Meeting of the American Society of Precision Engineering,* 2021.

[18] J. Dietrich, Praxis der Zerspantechnik, Wiesbaden: Springer Fachmedien, 2016.